7 CONTROL OF STRAY LIGHT

Robert P. Breault
Breault Research Organization
Tucson, Arizona

7.1 GLOSSARY

A	area
BRDF	bidirectional reflectance distribution function
GCF	geometric configuration factor
L	radiance
R	distance
θ, ϕ	angles
Φ	power
Ω	solid angle

7.2 INTRODUCTION

The analysis of stray light suppression is the study of all unwanted sources that reduce contrast or image quality. The control of stray light encompasses several very specialized fields of both experimental and theoretical research. Its basic input must consider (1) the optical design of the system; (2) the mechanical design, size, and shape of the objects in the system; (3) the thermal emittance characteristics for some systems; and (4) the scattering and reflectance characteristics of each surface for all input and output angles. It may also include spectral characteristics, spatial distribution, and polarization. Each of these areas may be concentrated on individually, but ultimately the analysis culminates in the merging of the various inputs.

Developments in detector technology, optical design software, diffraction-limited optical designs, fabrication techniques, and metrology testing have created a demand for sensors with lower levels of stray radiation. Ways to control stray light to meet these demands must be considered during the "preliminary" conceptual design. Decisions made at this time are, more often than not, irrevocable. This is because parallel studies based upon the initially accepted starting design are often very expensive. The task of minimizing the stray radiation that reaches the detector after the system has been

designed by "adding on" a suppression system is very difficult. Therefore, every effort should be made to start off with a sound stray light design. To ensure a sound design, some stray light analysis should be incorporated in the earliest stages of a preliminary design study.

This chapter presents some basic concepts, tools, and methods that you, the optical or mechanical designer, can consider when creating a sensor system. You do not need to be very experienced in stray light suppression to design basic features into the system, or to consider alternative designs that may significantly enhance the sensor's performance. The concepts are applicable to all sizes of optical instrumentation and to virtually all wavelengths. In some cases, you can use the concepts to rescue a design when experimental test results indicate a major design flaw.

7.3 CONCEPTS

This section outlines some concepts that you can use to reduce stray radiation in any optical system. The section also contains some experimental and computer-calculated data as examples that should give you some idea of the magnitude of the enhancement that is possible.

The power on a collector depends on the following:

1. The power from the stray light source.
2. The surface scatter characteristics of the source; these characteristics are defined by the bidirectional scatter distribution function (BSDF).
3. The geometrical relationship between the source and collector. This relationship is called the geometrical configuration factor (discussed later in this section).

To reduce the power on the detector, we can try to reduce the contributions from these elements:

$$\Phi_{\text{collector power}} = \Phi_{\text{source power}} \times \text{BRDF}_{\text{source}} \times \text{GCF}_{\text{source collector}} \times \pi \tag{1}$$

Ways to reduce each of these factors are discussed below. The creative use of aperture stops, Lyot stops, and field stops is an important part of any attempt to reduce the GCF term of the power transfer equation.

For the discussion that follows, examples from a two-mirror Cassegrain design, with the aperture stop at the primary, will be used to stimulate thoughts about stray light reduction possibilities for other sensors.[1] The system is shown in Fig. 1.

Critical Objects

The most fundamental concept is to start the stray light analysis from the detector plane of the proposed designs. The most critical surfaces in a system are those that can be seen from the detector position or focal surface. These structures are the only ones that contribute power to the detector. For this reason, direct your initial attention toward minimizing their power contributions by removing them from the field of view of the detector.

The basic idea is to visualize what would be seen if you were to look out of the system from the image plane. Unlike most users of optical instruments, the stray light designer's primary concern is seldom the object field, but rather all the interior surfaces that scatter light. It is necessary to look beyond the radii of the imaging apertures to find the sources of unwanted energy. Removing these sources from the field of the detector is a real possibility, and will result in a significant improvement in the system.

Real-Space Critical Objects

I will start out by identifying a particular critical real-space object that can be seen by the detector in our example; it is the inside of the secondary baffle. The direct view discussed here is different than the image of the same baffle reflected by the secondary which is discussed in the next section.

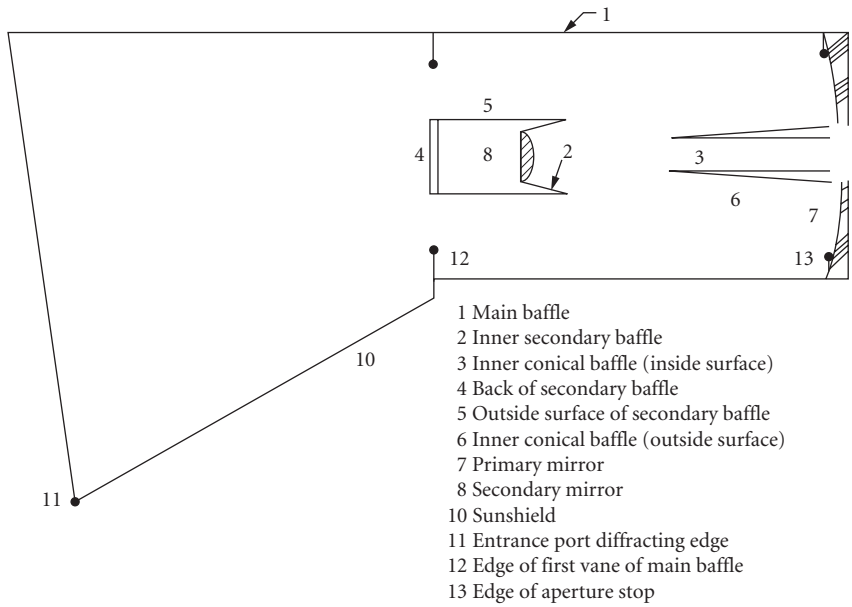

FIGURE 1 Typical Cassegrain design with the aperture stop at the primary. (*Ref. 2, p. 52.*)

Many Cassegrain secondary baffles have been designed to be cone-shaped (Fig. 2), usually approximating the converging cone of light from the primary. From the detector, portions of this secondary cone are seen directly as a critical surface. Since most of the unwanted energy is incident on this baffle from nearly the same direction as this surface is seen from the detector, the addition of vane structures would be of little help, assuming an optimum coating is used on the simple baffle. If the cone is made *more* cylindrical, the amount of critical cone area is reduced, and the angle at which the surface is seen gives a smaller projected area (Fig. 3).

Avoid making the baffle cylindrical because the outside of it would be seen. Since the detector is of a finite size there is a fan of rays off the primary representing the field of view of the telescope.

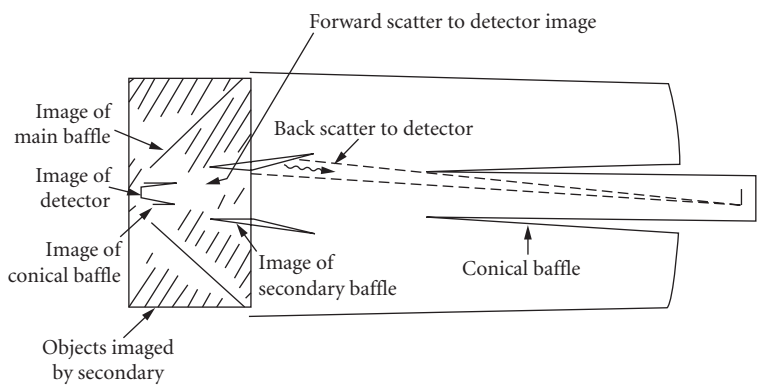

FIGURE 2 Direct and reflected scatter from the cone-shaped secondary baffle. (*Ref. 1, p. 4.*)

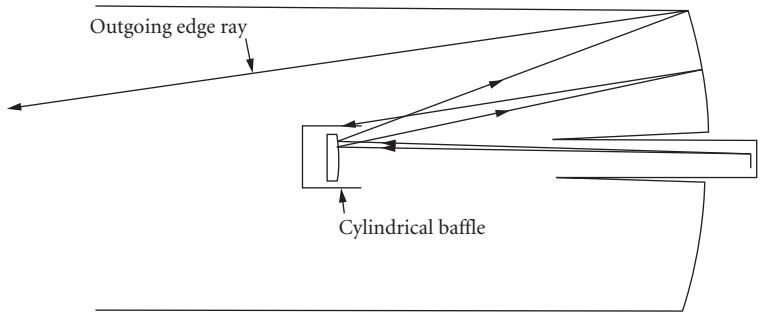

FIGURE 3 Reduced scatter from an almost cylindrical-shaped secondary baffle.

Although collimated for any point on the detector, any point not on axis would have its ray bundle at some angle to the optical axis, hence a cylindrical secondary baffle would be seen from off-axis positions on the detector.

Imaged Critical Objects

Imaged objects are often critical objects. They too can be seen from the detector. Determining which of the imaged objects are critical requires a bit of imagination and usually some calculations; stray light software can help you make the calculations. The Y-Y bar diagram can help you to conceptualize and determine the relative image distances and sizes with a minimum number of calculations.[3] The same could be done with other first-order imaging techniques (see Chap. 1 in this volume). Using the Cassegrain example again (Fig. 2), you can see that reflected off the secondary mirror are the images of the detector and the inside of the inner conical baffle (object 3 in Fig. 1). In some designs the outside of the conical baffle will be seen in reflection. These are *imaged critical objects*. If you wish, you can eliminate some of these images with a central obscuration on the secondary, or for the conical baffle, with a spherical mirror concentric about the image plane. The direct view to the inner conical baffle will remain, but the path from the image of it is removed.

The cone-shaped secondary baffle is also seen in reflection (Fig. 2). For the incident angles of radiation on this surface, the near specular (forward-scattering) characteristics will often be one of the most important stray light paths because the image of the detector is in that direction. This is an extension of *starting from the detector*. There is an image of the detector at the prime focus of the primary mirror. Often, as in this case, one location may be easier than another for you to determine what could be seen. By making the baffle more cylindrical, part of the *image* of the baffle is removed from the detector's view; as a result, the power that can scatter to the detector is reduced. Furthermore, it is sometimes possible to baffle most of this power from the field of view with one or two vanes (Fig. 4).

Continue the process of removing critical surfaces until all the critical surfaces have been considered for all points in the image plane. The power contributions from these surfaces will either go to zero, or at least be lessened after you reduce the area of the sections seen.

There is still more that can be done, since only the GCF term in the power transfer equation to the detector has been reduced. It is also possible to minimize the power onto the critical sections, which will become the source of power, Φ, at the next level of scatter. This approach can be very similar to the approach used for minimizing the power scattered to the image plane. The viewing is now forward from the critical surfaces instead of the image plane. By minimizing the BRDF and GCF factors of the surface scattering to the critical sections, the power incident on the critical surfaces will be reduced. Hence, the power to the detector is also reduced.

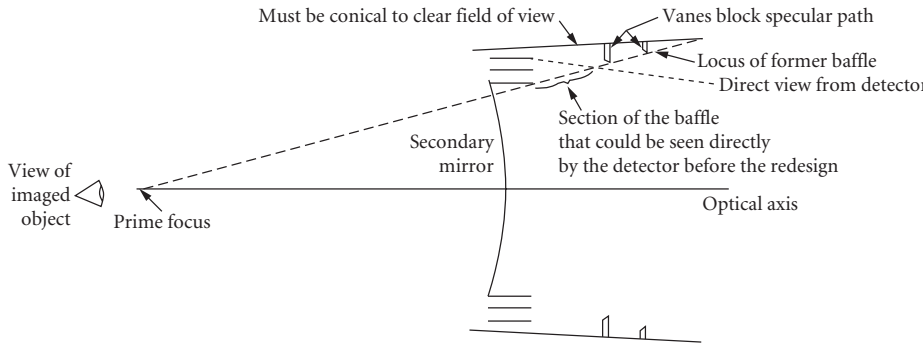

FIGURE 4 A cylindrical secondary baffle can be seen from off-axis positions on the detector.

Illuminated Objects

Minimizing the GCFs and BRDFs for the specific input and output angle is sometimes easier if you look into the system from the position of the stray light source in object space. By doing this, you can identify the surfaces that directly receive the unwanted energy. I will call these the *illuminated objects*. If any of these illuminated surfaces contain sections that the detector can see, then you should direct your initial efforts toward eliminating these paths. These paths will usually dominate all other stray light paths because there is only a single scatter before the stray light reaches the detector. An example of such a path that is often encountered is from the source onto the inner conical baffle of multimirror systems (Fig. 1). Some of the ways that the direct radiation can be eliminated is by extending the main baffle tube, increasing the obscuration ratio by increasing the diameter of the secondary baffle (Fig. 5), or by narrowing the field of view, which will allow you to extend the secondary baffle and the inner conical baffle toward each other.

The effect of eliminating this path is shown in a composite Point Source Transmittance (PST) plot in Fig. 6.[4] The PST plot is defined as the reference plane (detector plane in most cases) irradiance divided by the input irradiance along the line of sight. (See the section called "Point Source Transmittance Definitions" for a more detailed definition of PST.) For the case shown, the unwanted irradiance on the detector is reduced by over an order of magnitude.

Aperture Placement

I will now focus on the optical design aspects of a stray light suppression system, and give a qualitative discussion of some general aspects that you might consider. All optical systems will have at least

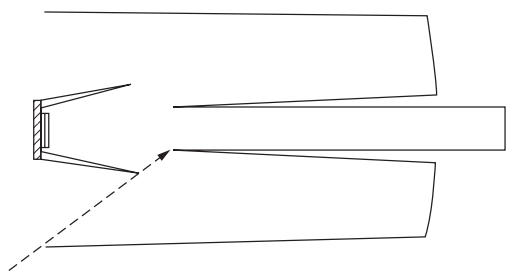

FIGURE 5 Increased obscuration ratio blocks direct path to inner conical baffle. (*Ref. 1, p. 6.*)

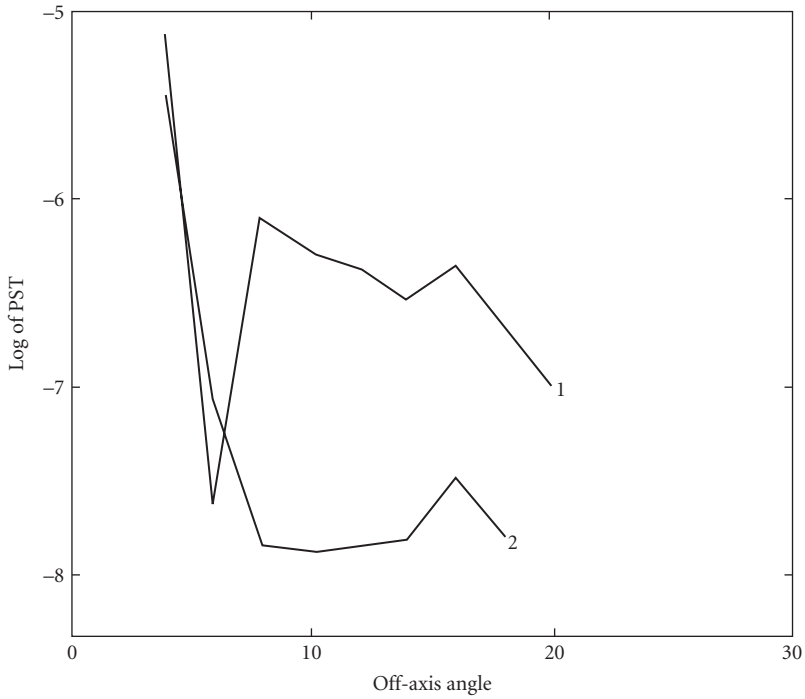

FIGURE 6 Point source transmittance with obscurations of (1) 0.333 and (2) 0.4. The 0.4 obscuration removed the direct path from the source to the inner conical baffle. (*Ref. 1, p. 6.*)

one aperture, called an *aperture stop*, that limits the size of the bundle of the incoming signal rays. Some systems will have field stops and/or Lyot stops. Each type of stop has a clearly defined role in stray radiation suppression, which is discussed in the following sections.

In many cases stop placement will have a much more noticeable effect on system performance than any vane structure, coating, or baffle redesign. Probably the only factor with more effect on the PST curve is the off-axis position of the source. Therefore, the benefits of any of the stops cannot be overemphasized.

Aperture Stops The aperture stop is the aperture that limits the size of the cone of radiation that will reach a point on the image plane. Sometimes shifting this stop allows the optical designer to better balance the aberrations. In a stray radiation suppression design, it plays a similar important role. All objects in the spaces preceding the stop in the optical path will not be seen unless they are imaging elements, central obscurations, or objects that vignette the field of view. Only a limited number of critical objects is possible before the aperture stop. In the intervening spaces from the stop to the image plane it is likely that many of the baffle surfaces will be seen. Figure 7 represents a two-mirror design, and Fig. 8 represents a three-element refracting system; both have the stop at the first element. In both cases the second element is oversized to accommodate the field of view from a point in the field stop; the amount depends on the full field of view of the design. Because the elements are oversized, the main baffle following the first element will be seen. This baffle will be a critical object, a direct path of unwanted energy. The "overviewing" is characteristic of all of the optical elements past the aperture stop.

If you move the stop along the optical path toward the detector plane, its performance as a stray radiation baffle will improve. If you shift the stop to the second element, the intermediate baffle will

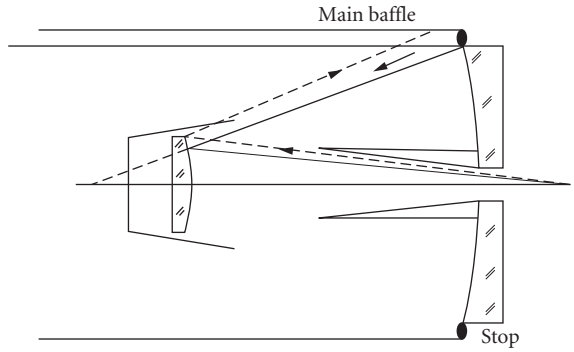

FIGURE 7 The oversized secondary allows the main baffle to be seen in reflection. (*Ref. 1, p. 8.*)

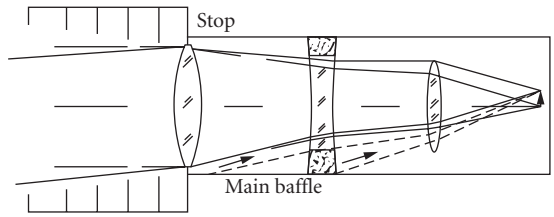

FIGURE 8 The main baffle is seen through the oversized secondary and tertiary. (*Ref. 1, p. 8.*)

not be seen. It is removed from the field of view of the detector, since the stop now eliminates direct paths from baffles in all spaces that precede it. Figure 9 shows the improvement in the PST curve for a two-mirror system. By moving the stop you have reduced the PST by a factor of 10. This is a desirable feature to consider for stray radiation reduction.

Direct paths from central obscurations can be blocked by a central disk located at some location deeper into the system; however, because of the parallax involved between the central obscuration disk and this central disk, the central disk obscuration will usually be a larger obstruction to imaging rays. In a reimaging design it is often possible to locate a central disk conjugate to the actual central obscuration.

Field Stops An aperture can be placed at intermediate *images* in a system to limit the field of view. Such an aperture will usually prevent any stray light from outside of the field of view from being directly imaged into the system beyond this field stop aperture. In a sense, its operation is just opposite that of an aperture stop. Baffle surfaces following a field stop cannot be seen from outside the field of view in the object plane, unless they are central obscurations. Note that with just a field stop, succeeding optical elements may allow out-of-field critical sections to be seen *through* the field stop, from within the field in the image plane (Fig. 11). Aperture stops are necessary to block such paths. Figures 10 and 11 show two such cases. Although for some designs the field stop is not 100 percent effective because of optical aberrations, its small size limits most of the unwanted stray light. Field stops therefore do not remove critical sections, but rather limit the propagation of power to illuminated objects. In reflecting systems, take care that the object side of the field stops does not become a critical area, which can be seen directly or in reflection from the image plane because unwanted energy is being focused onto them.[5]

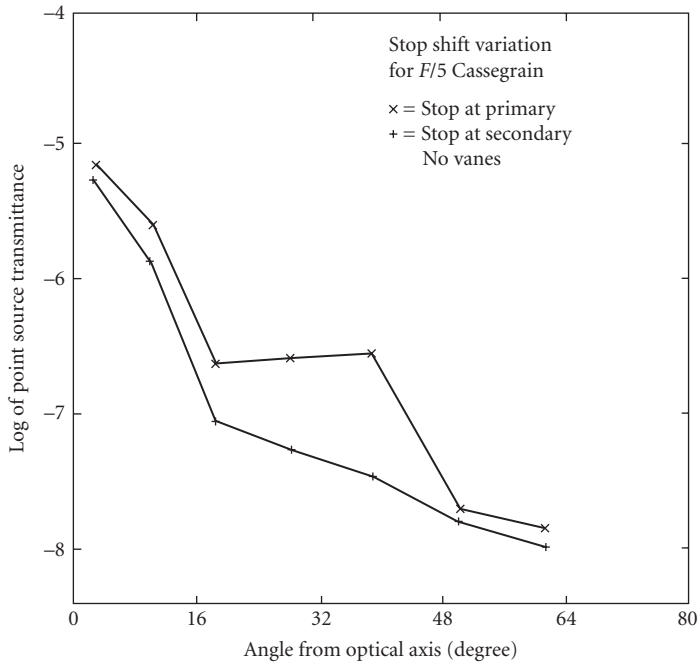

FIGURE 9 PST improvement with stop shift for the two-mirror system. (*Ref. 1, p. 8.*)

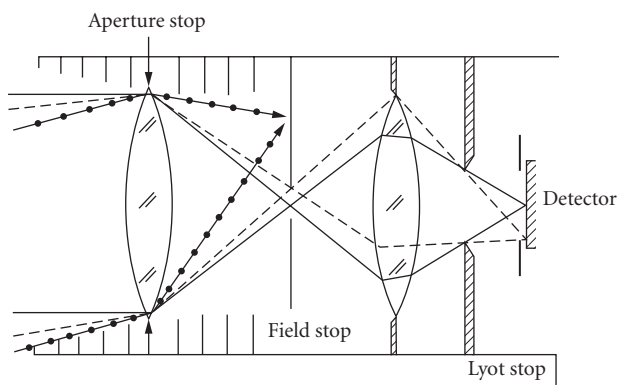

FIGURE 10 The addition of a Lyot stop prevents preceding baffles from being seen from the image.

Lyot Stops A limiting aperture placed at the location of the image of an aperture stop, sometimes called a glare stop or Lyot stop, has the same property as described for aperture stops. It should be slightly smaller than the image of the aperture stop. It limits the critical sections which are out of the field of view to those objects in succeeding spaces only. Since Lyot stops are by definition further along the optical path to the detector, the number of critical surfaces seen by the detector will be reduced. Usually, these stops are incorporated into the design to block the diffracted energy from an aperture stop and field stop pair, so that only secondary or tertiary diffracted energy reaches the image. Nevertheless, both diffracted and scattered energy are removed from the direct

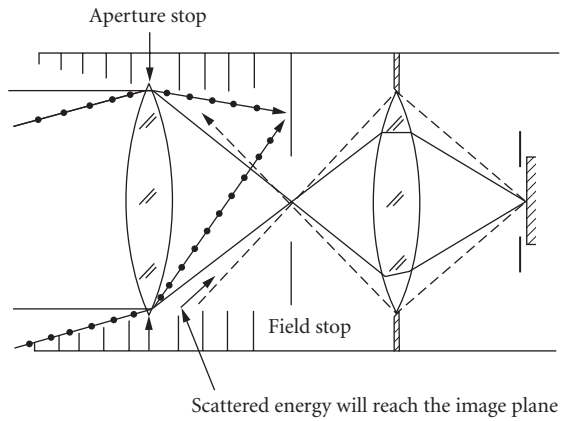

FIGURE 11 Out-of-field energy in object plane will not be imaged beyond field stop. Out-of-field energy elsewhere may be seen. (*Ref. 1, p. 9.*)

view of the image, re imaging the largest optical element as the stop takes full advantage of both the light-gathering power of the optics and the stray radiation suppression features provided by the stop. Figure 10 shows a system with a Lyot stop.

On space-based telescopes the image plane is often *shared* by one or more instruments. Each instrument reimages the telescope's image through some optical train, and eventually onto the detector. In that optical train there could be a logical place to use a Lyot stop to improve the stray light performance of the viewing instrument well beyond that of the telescope.

It is the combination of these different stops or apertures that helps minimize the propagation of unwanted energy by limiting the number of critical objects seen by the detector, and the objects illuminated by the stray light source.

When all direct paths have been eliminated, the next step is to determine the relationship between the sections that received power (illuminated objects) and the critical surfaces. This relationship takes the form of scattering *paths*; that is, stray light can scatter from the illuminated objects to the critical objects. To start reducing the stray light contributions from these paths, you can start at the critical surfaces as described above. But now you have more knowledge about where the direct incident power is being distributed throughout the system, since you can also look into the system from the source side to find the surfaces receiving direct power. With this information you can identify the possible paths between the illuminated and critical surfaces.

Design considerations for extended baffle shields (Figs. 12 and 13) provide a good example of starting from the source side to identify possible paths. In the examples, object 2 (an optical surface) is the largest contributor of scattered radiation and is the best superpolished mirror available

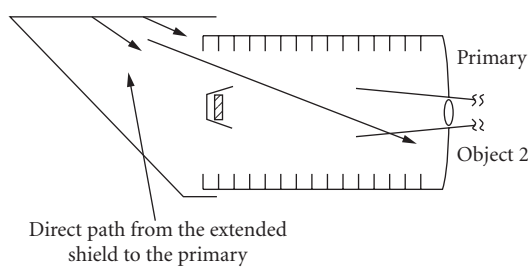

FIGURE 12 There is a direct path from the baffle to the primary mirror. (*Ref. 1, p. 7.*)

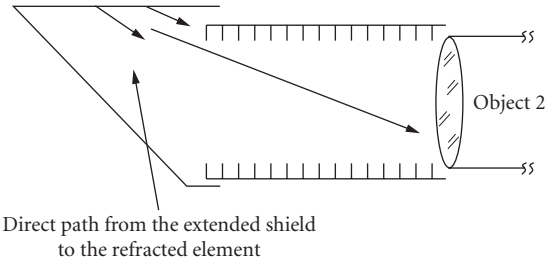

FIGURE 13 There is a direct path from the baffle to the refracting element. (*Ref. 1, p. 7.*)

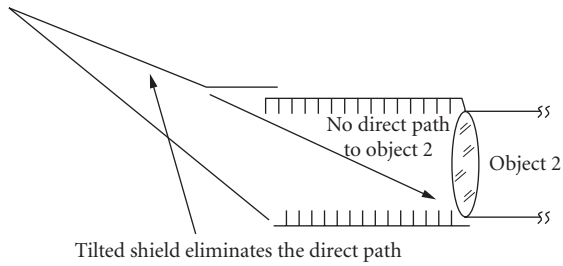

FIGURE 14 Direct paths are removed by properly tilting the shield. (*Ref. 1, p. 7.*)

(Fig. 12), or if it is a lens as in Fig. 13, it has the lowest possible scattering characteristics. It cannot be removed from the view of the image plane. If the initial power incident on object 2 is only from the extended shield, then by tilting the shield (Fig. 14), the power on the shield must first scatter to the main tube and then to the optical element. The combination is then referred to as a two-stage baffle. If vanes are added to the main baffle, the scattered radiation incident on the optical element will be reduced by many orders of magnitude when all the scattering solid angles and the number of absorbing surfaces are considered. Note that without the tilt to the shield, vanes on the main baffle are worthless because there is a direct path to the objective.

Figure 15 is an abstract representation of the process of reducing stray light in a sensor system. Start at the detector, then work from its conjugate image locations. Starting from the detector simplifies the analysis and directs your attention to the most productive solutions, because you can identify all the possible sources of stray light to the detector. You can then work at decreasing their number by slightly redesigning the baffles and stops. Next, identify which objects are illuminated. Discover how energy may propagate between them and you have identified the paths of stray light propagation. From then on the process of moving objects or blocking paths is quite simple, although the quantitative calculations might get difficult and may require some analysis software.

Baffles and Vanes

A few definitions are required to define baffles and vanes. Other authors have used their own different definitions. In this section the term *baffle* is used to describe conical structures (including cylindrical) that can also be described as tubelike structures. Their function is to shade, or occult, stray light from the source to one or more system components. The main baffle shields the primary

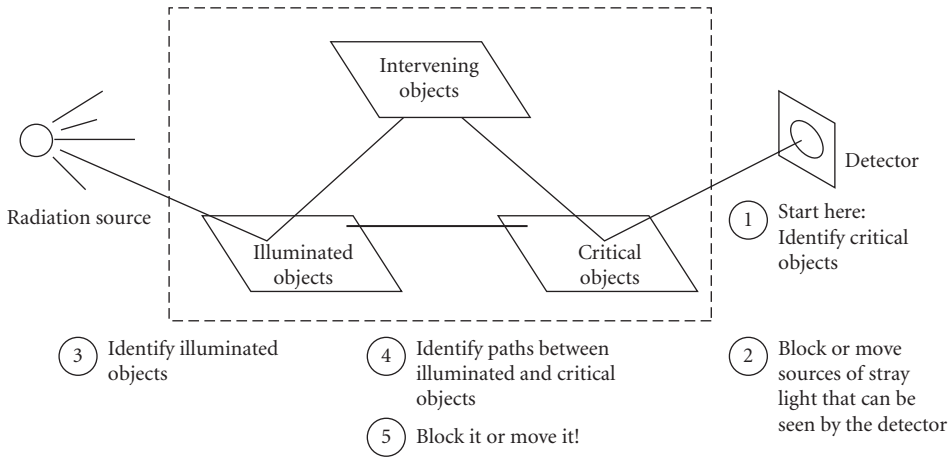

FIGURE 15 The first step in a stray light analysis begins from the detector plane, not from the source.

mirror from direct radiation at the larger off-axis angles. *Vanes* are structures put *on* baffles to affect the scatter characteristics of the surface. Other authors have used the term "baffles," or "glare stops," to describe these vanes.

Baffles In a well-designed system vanes play an important role only at large off-axis angles. For example, when one-tenth of the stray light falls on the primary of the Cassegrain design, then the main baffle receives the remaining 90 percent of the stray light. When the main baffle has properly designed vanes on it, light that falls on the baffles is attenuated by five orders of magnitude before it reaches the primary mirror. The resultant power on the primary mirror is then about 9.0×10^{-5} compared to the direct 10 percent that fell on the mirror. This results in less than 0.1 percent of the total on the primary. In addition, most of the subsequent scatter off the primary will be at much higher scatter angles. This will cause the scattered energy to have much lower BRDFs off the primary mirror when scattered in the direction of the detector, further reducing the scatter contribution from the baffle.

Only when no power illuminates the objective will the baffles play a significant role in the propagation paths of the stray light. Usually the system's performance merit function is then very good. Only if the stray light source has a tremendous amount of energy, like the sun, does the stray light become measurable.

Vanes The depth, separation, angle, and bevel of vanes are variables that need to be evaluated for every design. In the following paragraphs stray light analysis results are presented for both a centrally obscured system (Cassegrain) and an unobscured eccentric pupil design (Z-system).[6] Profiles of these systems are given in Figs. 2 and 16. Of the two designs, only the eccentric pupil design has a reimager that would allow for the placement of an intermediate field stop and an accessible Lyot stop, as discussed above.

The APART stray light analysis program was used to analyze the two designs. The APART program was a substantial software package that performed deterministic calculations of stray light propagation in optical systems.[2,7,8]

As an example of vane design considerations, the design of vanes on a main baffle tube will be explained. With minor differences, the design steps are the same for the Cassegrain and the eccentric pupil designs. In a reimaging system, vane structure deep in the system is usually not necessary, but there are exceptions. Figure 17 shows a collecting optical element that has some small field of view (FOV). The optical element could represent a primary mirror or a refractive element.

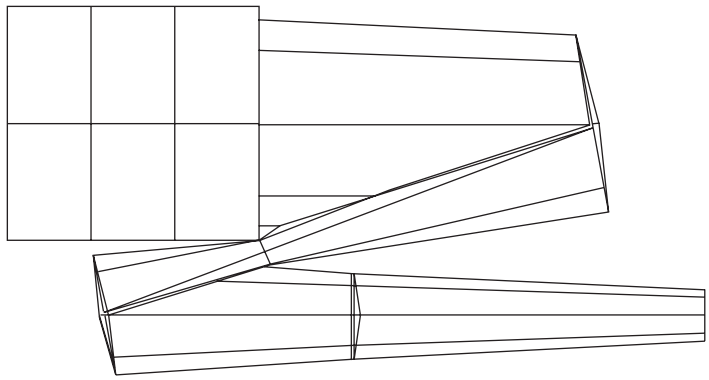

FIGURE 16 Confocal mirror system, eccentric pupil, no obscuration, low-scatter system. (*Ref. 6, p. 91.*)

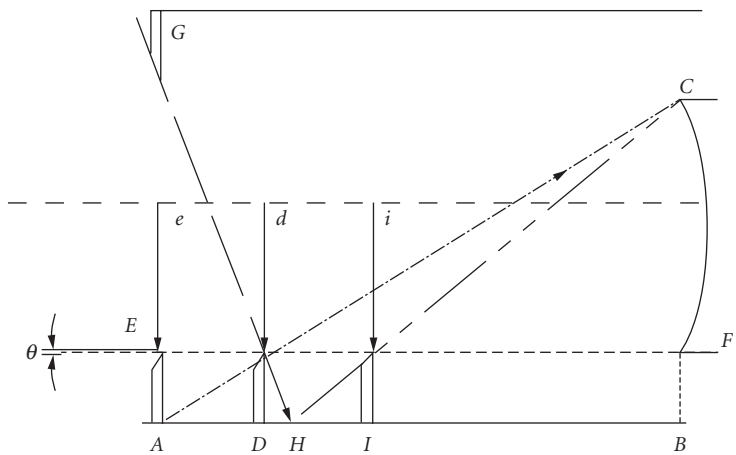

FIGURE 17 Vane placement design, lowercase letters are radii (measured from the optical axis), uppercase are *z* locations. (*Ref. 6, p. 94.*)

The placement of a straight, diffusely coated cylindrical tube would block the direct radiation from an external source, such as the sun, from reaching the optical element for a certain range of off-axis angles. If it were at a large off-axis angle, the forward scatter off the inside of the tube would be so high that it would normally not be acceptable. The solution is to add vanes to block this path.

Figures 18 and 19 depict the two cases that could represent the scatter from a baffle. In one case there are no vanes; in the other case there are vanes. This example shows how a propagation path is blocked by vanes. Vanes are useful, but a better approach is to make the solid angle (Ω_c) from the baffle (not the vanes) to the collectors of the scattered light go to zero, so that there is no path from the baffle and vane structure to the collecting object. By moving the baffle out of the field of view of the collector, the baffle's contribution goes to zero. There is no edge scatter, and no edge diffraction effects. That topic is in the realm of baffle design, which has already been touched on, and is well covered in the literature.[9,10]

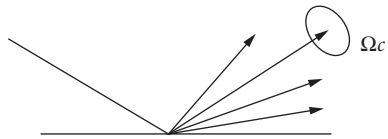

FIGURE 18 High forward scatter path. (*Ref. 6, p. 92.*)

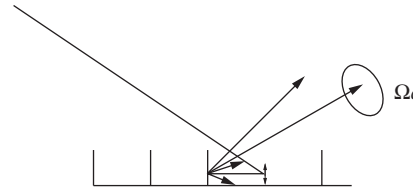

FIGURE 19 Forward scatter path highly attenuated by the vane structure. (*Ref. 6, p. 92.*)

Designing the Vane Spacing and Depth[11]

A first vane is most often placed at the entrance of the baffle and an external ray is brought in from object space at a maximum off-axis position. If there is no forebaffle the angle is 90° off axis. The depth of the vane cavity is normally dictated by space and weight requirements. Too little depth will dictate the requirement for many vanes. Then vane edge scatter eventually becomes the major source of scatter instead of multiple vane scatter.

The initial ray will strike the side wall at the base of the first vane (point *A* in Fig. 17). From this point, a design line is drawn/calculated (*AC*) from the wall to the edge of the optical element on the opposite side. This line (*AC*) intersects the edge ray (*EF*), at *z* position *D*. At this point a vane could be placed. Mathematically, this assures that any point below *C*, including those on the optical element, would not see any directly illuminated side wall. However, practicality dictates that some offset of point *D* to a point *D′* (not shown) is required to allow for tolerance errors in fabrication of the vane, thermal effects, assembly errors, and for stray light edge scatter and diffraction effects. The tolerance allowance is company-, material-, and design-dependent. Acceptable numbers are often about 0.125 mm for fabrication and assembly tolerances. For the rest of this analysis, assume that this is accounted for.

Continue the design process by constructing another line from the edge of the entrance aperture to the tip of the second vane to the wall (line *GH*). Draw a new *HC* line to the area near the objective and determine the placement of the third vane (at *I*); once tolerances are considered, iterate the process to reach a final design. In some cases you may have to consider more than just the scatter path to the objective. In the Cassegrain design you may also have to consider the inner conical baffle opening. It is beyond the present scope to go into further detail.[12]

Bevel Placement on Vanes In this short discussion on baffle-vane design and placement, I did not mention the placement of a slanted surface, or bevel, sometimes placed on a vane edge as shown in Fig. 20. Which side should the bevel go on? The answer is usually dictated by first-order scatter principles.[13,14] Near the front of the tube, direct radiation from a source at large off-axis angles will strike this bevel. If it is placed on the right side (Fig. 21), then the illuminated bevel will scatter its radiation all the way down into the tube to some optical surface. If placed on the left side, as depicted in Fig. 20, then it will go only 16° deeper into the system to the opposing vanes, a much better solution. For vanes deeper into the system, the bevel is placed on the right side. The point at which this is done is determined by the angle of the bevel and the diameter of the baffle tube. At some point, external radiation will not be able to directly strike the beveled edge if it is on the right-hand side of the vane. Only the nonbeveled, straight side will be illuminated. Therefore, the vane can rescatter only in the left side of the hemisphere, which is in the direction of going out of the system. If the bevel is placed on the left side, it can scatter 16° (in the example) deeper into the sensor; this is usually a needless design shortcoming that could be a significant error.

Vane Angle Considerations Another variation on the design feature of vanes that has sometimes been incorporated onto baffles in an optical system is angled vane structure. These vanes are nonplanar objects. This makes them quite tedious to cut out of sheet metal, fabricate, and install.

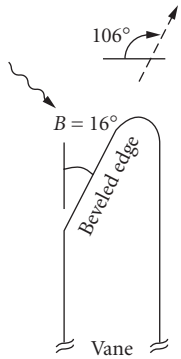

FIGURE 20 Placement of the bevel on the left side of the vane structure. (*Ref. 6, p. 96.*)

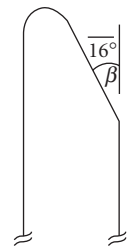

FIGURE 21 Placement of the bevel on the right side of the vane structure. (*Ref. 6, p. 96.*)

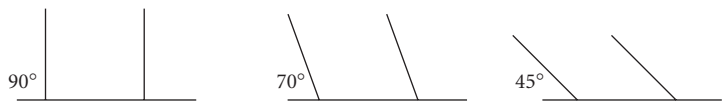

FIGURE 22 Vane structure angled at 90, 70, and 45°, respectively. (*Ref. 6, p. 97.*)

The next few paragraphs will present computer analysis results from two designs to show the effect of vanes on the propagated stray light. The vane angles used were 90, 70, and 45°, as depicted in Fig. 22.

The comparative stray light results for the Cassegrain system (Fig. 1) with a Martin Black coating on the vanes are shown in Fig. 23; in this system the vanes are on the main baffle, but not on the sunshade. There is no difference in the performance as the vane angle is varied from 45° to 90° (all three curves lie one on top of the other).

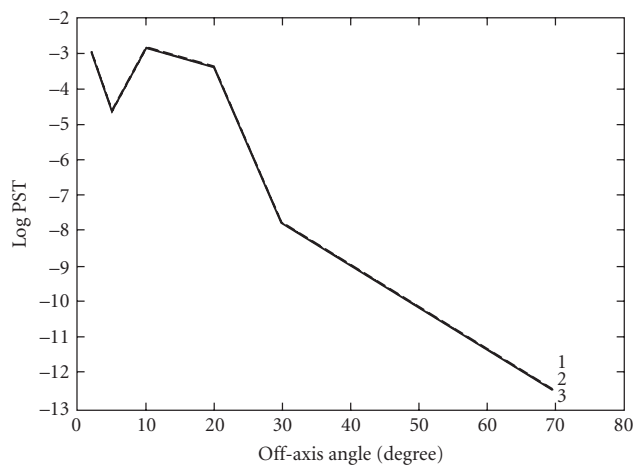

FIGURE 23 Cassegrain with Martin Black. Vane angles 1 = 90°, 2 = 70°, 3 = 45°. Log PST = detector irradiance divided by input irradiance. (*Ref. 6, p. 97.*)

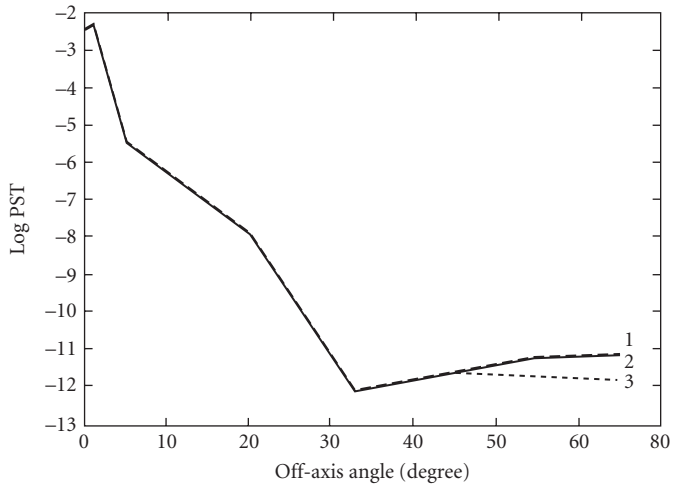

FIGURE 24 Z-system with Martin Black. Vane angles 1 = 45°, 2 = 70°, 3 = 90°. Vanes are on the sunshield. (*Ref. 6, p. 114.*)

The comparative results for the Z-system (Fig. 16) with vanes on the sunshield are shown in Fig. 24. The results differ from the Cassegrain results for source located at angles greater than 45° off-axis. This is because the primary side of the baffle is illuminated and scatters light directly to the primary mirror. The 70° baffles would fail for sources beyond 70° off-axis. The Cassegrain system has vanes on the main baffle (not the sunshade) and the sunshade occulted the direct illumination of the primary side of the 45° vanes. This accounts for the subtle but important difference in the results.

Usually the first-order scattering properties of the vane structures are more important than whether the vanes are angled or not. The results presented above confirm this statement. There are occasions where angled vanes would be beneficial, but to fully understand those cases a much longer explanation of diffuse vane baffle scatter is necessary. These results are detailed elsewhere.[15,16]

There are special situations where angled vanes will have a significant advantage over annular vanes. One example is a bright source at a fixed offset angle. I have seen such a feature on a space-borne telescope on a platform where there was nearby a brightly sunlit rocket-thruster casing at a fixed angle outside the field of view. Figure 25 shows the design where the vanes were aimed at the thruster at an angle where the primary mirror side (right side in Fig. 25) could not be directly illuminated by the sunlight scattered off the thruster. Under those circumstances most of the stray light

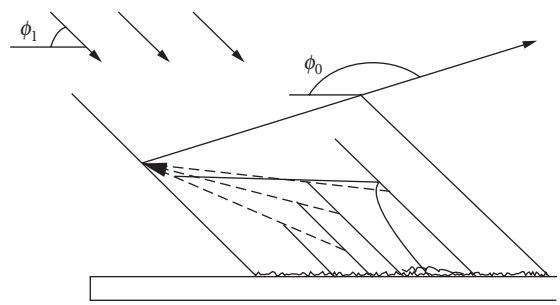

FIGURE 25 Angle-staggered vanes for fixed input angle. (*Ref. 6, p. 104.*)

had to make three scatters before exiting the vane cavity. In general, as soon as the position of the bright object is moved over a range of angles, the advantage of the angled vanes is lost. Nevertheless, there are many occasions within a sensor where the relative positions of a scattering source and a collecting object are fixed along a major stray light path. The front parts of the main-barrel baffle and the opening of the inner conical baffle in the Cassegrain design is an example. Many more examples could be cited. But the point is that you, as a designer, should first consider the first-order, single scatter paths off the baffle wall, each side of the vanes, and the bevel, for the full range of input values. Based on that information you can make the decision to user planar or angular vanes.

Vane Depth Considerations By varying the vane depth in the example analysis we can evaluate how the vane spacing-to-depth ratio affects system performance. Figure 26 gives the results of an analysis of the Cassegrain system with varying vane depths on the main baffle of 0.2, 0.4, and 0.8 inches. Figure 27 gives similar output from the Z-system analysis results. The performance of the system gets better as the vane depth increases from 0.2 to 0.4 inches, but there is little performance difference between the 0.4- and 0.8-inch baffle depths. The latter is the normal case. The 0.2-inch vane depth allows for a single path from the walls of the baffle tube, which increases the stray light propagation. Once that path is blocked by a greater vane depth, no further improvement should be expected due to further increases in vane depth.

The intent of presenting the two different optical designs was not to trade off one optical design against another. It needs to be made clear that the two optical sensors being used as examples are intentionally not equivalent from stray light design considerations. This is why the changes in performance are design-dependent. The nominal design of the eccentric pupil has a reimager, and the Cassegrain does not. The Cassegrain could have a reimager, in which case the stray light performance of both could be made essentially equal. It would depend on the optical design characteristics, F/#, field of view, obscuration ratio, etc. The Cassegrain design has a specular sunshield and the Z-system has a vaned diffuse baffle structure. Which would perform better could only be determined after all of these features are considered.

To summarize, the general points being made in this section are

1. Usually, angled vane structure has little, if any, additional benefit over straight, annular vanes, and the annular vanes are much easier to fabricate and assemble.
2. Once the depth of a diffuse black vane structure is deep enough to block the single scatter path, further increases will not improve performance.

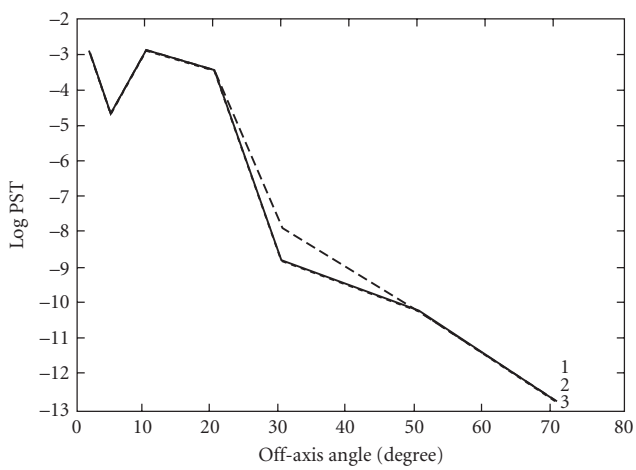

FIGURE 26 Cassegrain 90° baffles, coated with Martin Black, at varying depths; 1 = 0.2-inch, 2 = 0.4-inch, 3 = 0.8-inch depth. (Scatter is dominated by baffles.) (*Ref. 6, p. 98.*)

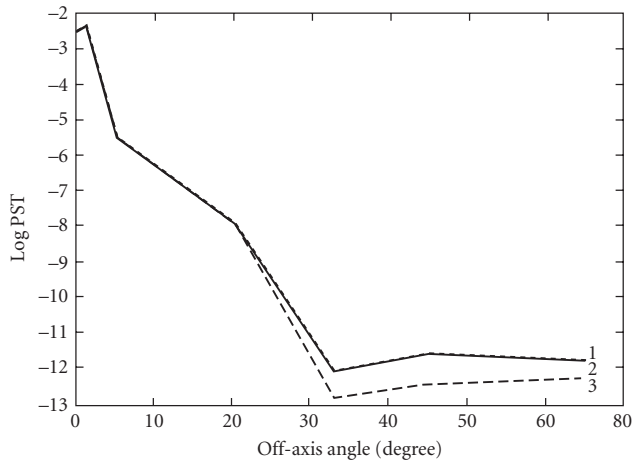

FIGURE 27 Z-system with varying vane depths. 1 = 0.2-inch, 2 = 0.4-inch, and 3 = 0.8-inch depth. (*Ref. 6, p. 114.*)

Specular Vanes Another aspect about vane structure that has been explored, but only in a limited way, is the specular vane cavity. Previous studies indicated that specular vanes have a problem with the aberrated rays and near specular angle scatter; this problem is severe enough to degrade the performance significantly.[17,18] In another study by Freniere this was not always true.[19] The ASAP[20] stray light software was used to evaluate the Z-system (Fig. 28) with (1) no vane structure, but with the main barrel baffle coated with Martin Black; (2) with Martin-Black-coated vanes; and (3) with a specular vane structure. The results show a dramatic degradation in the stray light performance without the coating on the main baffle tube. A subsequent specular baffle design developed by Nick Stavroudis has been shown to be a major improvement over previous concepts.[21]

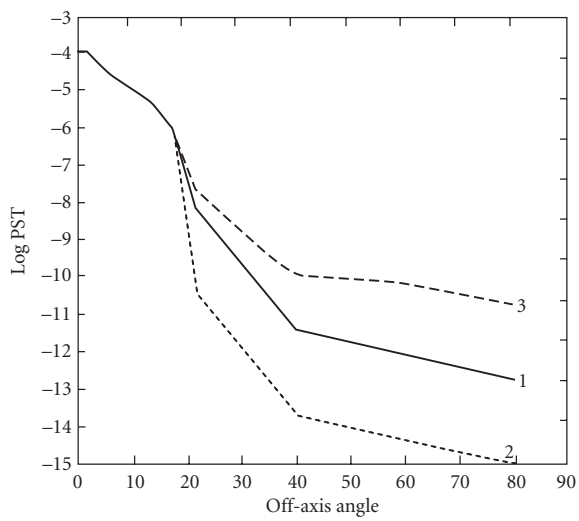

FIGURE 28 PST for unobscured pupil design without vane structure, with diffuse vane structure, and with specular vanes. 1 (solid) = no vanes, diffuse black coating; 2 (dotted) = diffuse vanes on main tube; 3 (dashed) = specular vanes on main tube. (*Ref. 6, p. 115.*)

Contamination Levels

Light scattered from a particulate-contaminated surface can have a pronounced effect on the stray light performance of a system.[22]

I will now relate the performance of both designs (the centrally obscured Cassegrain, and the unobscured eccentric pupil) as a function of the level of scatter, per MIL-STD 1246A.[23] This analysis evaluates the sensor for different amounts of contamination on the optics only. The levels of contamination as defined in IEST-STD-CC1246D are for a distribution of particles with a specified range in particle sizes.

Ray Young used Mie scattering theory to predict the BRDF of a mirror covered with such MIL-STD distributions.[24] Table 1 was generated from Young's work for the 10 μm radiation. This table shows the base BRDF value and the BRDF slope that would be used in a typical stray light analysis program for input. The base value is the BRDF value at $(\beta - \beta_0) = 0.01$ and the second term is the slope of the BRDF in a (log-log) plot of BRDF versus $(\beta - \beta_0)$. β_0 is the sine of the angle of incidence and β is the sine of the observation angle.[25] The terms work equally well for out-of-plane values, but the above definitions, for simplicity, assume in-plane scattering data. See also the works of Spyak.[22]

Spyak and Wolfe[26] did a series of experiments and calculations that relate BRDF to particulate contamination. They counted and sized particles on a mirror surface, and then measured the contribution of these particles to the mirror's BRDF at both visible (633 nm) and infrared (10.6 μm) wavelengths. They also performed Mie theory calculations and compared their calculations with the measured BRDFs. At both visible and infrared wavelengths, Mie theory calculations were a reasonable estimate for contribution of particulates to a mirror's BRDF. In most cases agreement between Mie calculations and their measurements were within a factor of two. Spyak and Wolfe also published Mie calculations of the BRDF expected from the MIL-STD-1246B (now IEST-STD-CC1246D) standard at 633 nm and 10.6 mm.*

Michael Dittman[27] has published a series of Mie calculations at five wavelengths. His calculations were done for the IEST 1246D distributions, but he considered an additional distribution in which the "particle slope" on the distribution was reduced from 0.926 to 0.383. The latter slope results in more large particles, and is commonly thought to be a more realistic distribution on surfaces that are exposed in a cleanroom environment.*

There is a problem with specifying the optics with this standard because it is difficult to reliably relate a level of contamination by particles to a BRDF performance. Two equal sizes and distributions of particulates may not give the same BRDF, because the index of refraction, the reflectivity, and the roughness of the particulates enter the calculations. In general, few people go to the trouble to determine these other factors. These factors will vary from one distribution to another. BRDF is the most usable value when performing a stray light analysis, so it should be the stray light specification. For manufacturing specifications, other parameters may be more appropriate, but they are not as good as BRDF for a stray light specification.

The level of scatter is also given in Table 1 along with the BRDF. The BRDF data from particulate scatter for the 5-, 10-, and 20-μm wavelengths for the 100, 300, and 500 contamination level have

TABLE 1 Mirror Scatter Relationships [Wavelength = 10 μm, BRDF Slope in Log $(\beta - \beta_o)$]

BRDF at $(\beta - \beta_o) = 0.01$	BRDF Slope	Cleanliness Level
0.02	–1.17	500
0.01	–1.17	454
0.001	–1.17	300
0.0001	–1.17	204
0.00001	–1.17	100

*Personal communication on partical contimination paragraphs, contributed by Dr. Gary Peterson, Breault Research Organization, Inc.

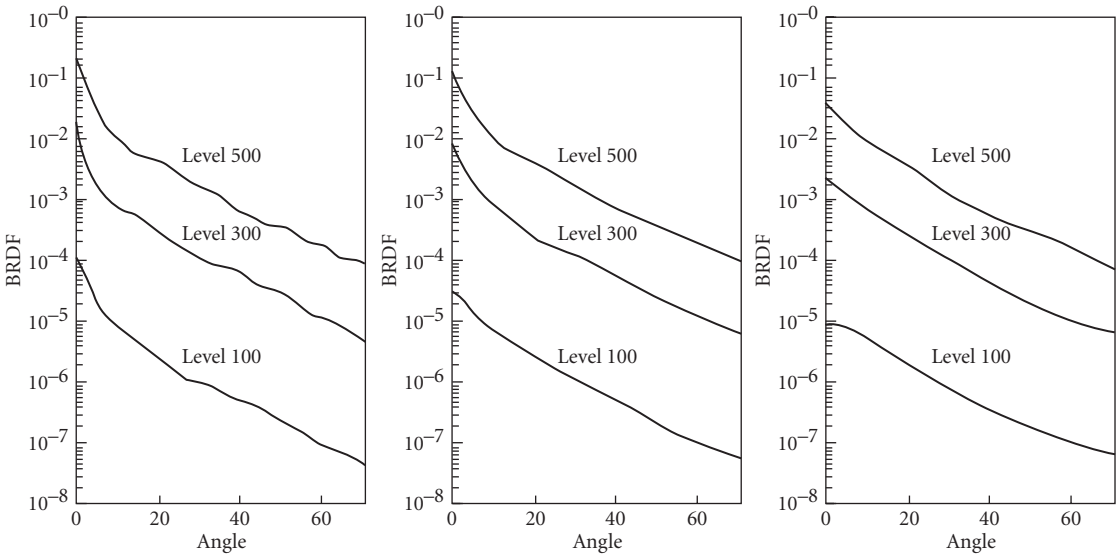

FIGURE 29 Predicted BRDFs on particles deposited on low–scatter mirror for cleanliness levels of 100, 300, and 500 at radiation wavelengths of 5.0, 10.0, and 20.0 μm.[24] (*Ref. 6, p. 105.*)

been plotted in Fig. 29. Consensus, not factually documented, indicates that the current state of the art of contamination control is at the cleanliness level of 300 to 500 for the 10-μm-wavelength region. Measured BRDFs below level 200 are achievable in the lab for short periods of time. A stray light analyst is strongly advised not to predict a system's performance with values below 1.0E-3 sr^{-1} in the 10-μm region. Based on historical performance, mirrors in the IR (10-μm region) consistently degrade to this value, usually because of particulate scatter. Research work performed under Rome Air Development Center contract for the detection, prevention, and removal of contamination from the ground and in space could greatly reduce the degradation currently experienced by IR sensors.[28]

Hal Bennett presents the significance of particulate scatter, as shown in Fig. 30.[29] This figure shows an agreement between measured data and theoretical data, and illustrates why IR sensors are usually more sensitive to particulate scatter than RMS scatter; the opposite is true in the visible. Figure 30 also indicates why the wavelength scaling law does not usually relate visible BRDF measurements to BRDF measurements in the IR. The physical process is different.

Figures 31 and 32 are the representative point source transmittances (defined as the irradiance on the detector divided by the incident irradiance) for the cleanliness levels of 100 through 500 for each design. The Cassegrain is much less affected by changes in contamination level, because the scatter from the black-coated surfaces dominates all other scatters. If the system had a reimager its performance would be better because these black surfaces would be blocked from the field of view of the detector, and the stray light performance would be due to the cleanliness level of the optics. The eccentric pupil design is sensitive to changes in the mirror coatings because it does have a reimager, and the major source of scatter is from the mirror surfaces.

In summary, the impact of particle contamination on the performance of a system will depend on how well the system is designed to suppress stray light. The goal is to be limited by a single optical element, such as the collecting lens or mirror, which is the objective of the system. The eccentric pupil design (Z-system) has this design feature. The better the optical design from a stray light point of view, the more the system's performance will be degraded by particle contamination. The more the system performance is determined by the black coatings, the more it will be sensitive to degradations in the coatings on the baffles.

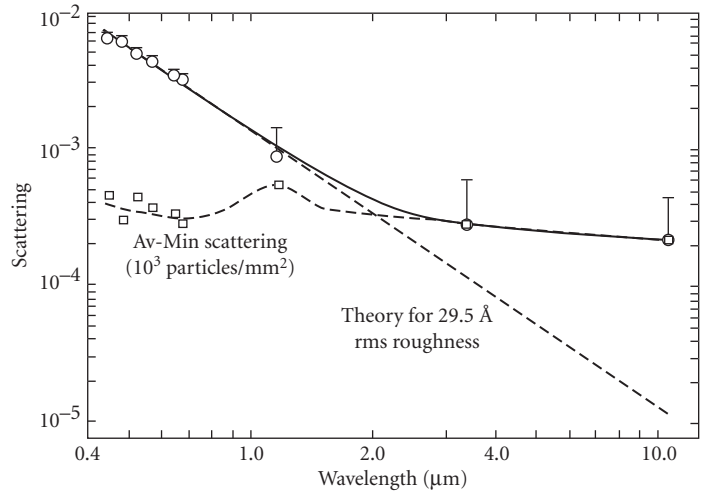

FIGURE 30 Scattering from polished dense flint glass. The diagonal line gives the contribution predicted for microirregularity scattering by a 29.5 Å rough surface. Circles indicate the minimum scattering observed, and the bars and squares the difference between the average and minimum scattering observed at several points on the surface. This difference may be related to particulate scattering. (*Ref. 29, p. 32.*)

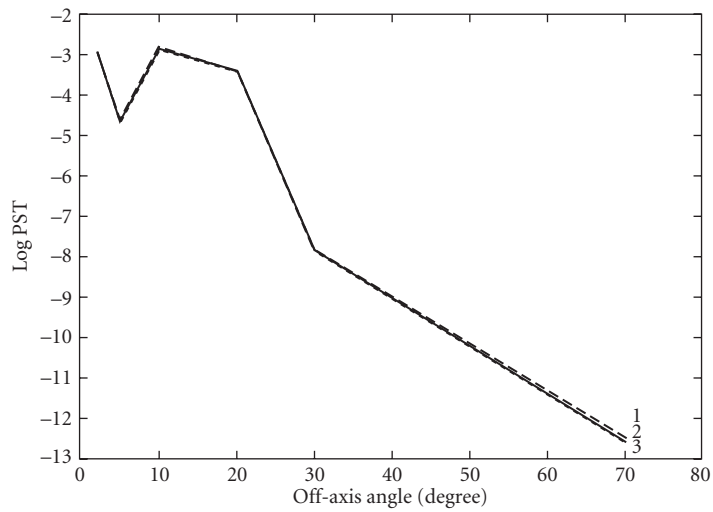

FIGURE 31 Cassegrain system with mirrors at all five contamination levels. 1 = 100, 2 = 204, 3 = 300, 4 = 454, 5 = 500. *(Ref. 5, p. 113.)*

Strut Design

In a centrally obscured system the central obscuration must be supported. In some designs (Schmidt-Cassegrains) the obscuration can be supported by a refractive element, but in most designs some form of struts are used. The most common error in strut design is to specify manufacture

CONTROL OF STRAY LIGHT 7.21

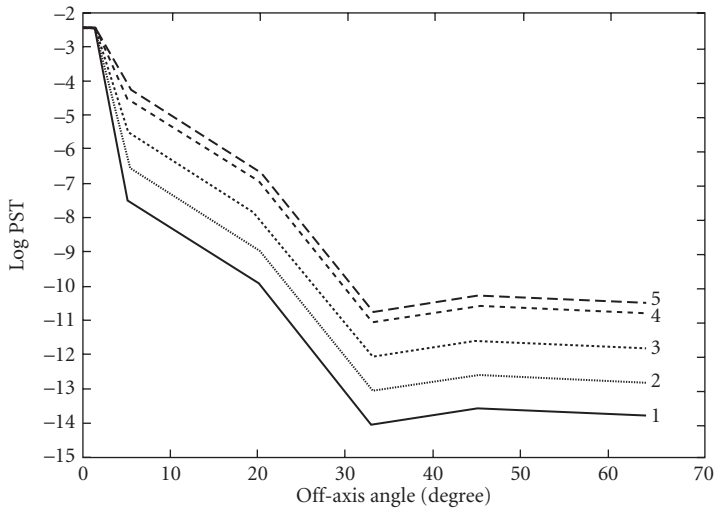

FIGURE 32 Z-system with mirrors at all five contamination levels. 1 = 100, 2 = 204, 3 = 300, 4 = 454, 5 = 500. (*Ref. 6, p. 113.*)

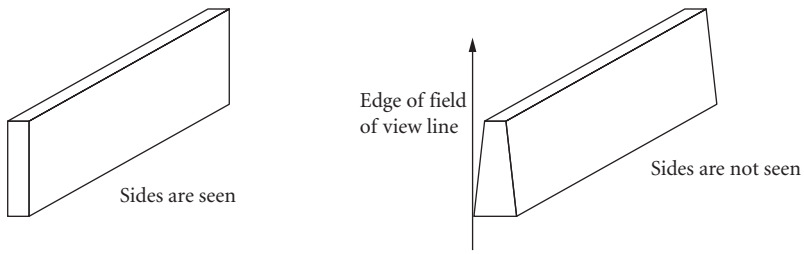

FIGURE 33 Angled strut design does not allow the detector to see the sides of the strut.

from a slab or plate of coated metal. Because all detectors have some finite field of view, the scatter from the sides of the struts can be seen from the image plane. Usually the struts are out "front" and exposed to more stray light sources than the objects deeper into the system. The near off-axis angles of incidence of scattered light off of the strut sides make for very high scattering toward the detector.

The proper strut design will preclude this path by making the object end of the strut narrower than the side nearest the objective (primary). This shape, shown in profile in Fig. 33, does not allow the detector to see the sides of the struts. The angle of the taper depends upon the object space field of view of the detector. It requires only a small change in design to remove this stray light path.

Basic Equation of Radiation Transfer

This section briefly discusses the most fundamental equation needed to perform the quantitative calculations of a stray light analysis. It reinforces the concept of first identifying what the detector can see and working on the geometry of the system to limit the stray light propagation, and not the BRDF term.

The fundamental equation relating to power transfer from one section to another is:

$$d\Phi_c = L_s(\theta_C, \phi_C)dA_s \frac{\cos(\phi_s)dA_c\cos(\phi_c)}{R_{sc}^2} \tag{2}$$

where $d\Phi_c$ is the differential power transferred, $L_s(\theta_C, \phi_C)$ is the radiance of the source section, dA_s and dA_c are the elemental areas of the source and collector, and ϕ_s and ϕ_c are the angles that the line of sight from the source to the collector makes with their respective normals. This equation can be rewritten as three factors that help clarify the reduction of scattered radiation.

$$d\Phi_c = \frac{L_s(\theta_C, \phi_C)}{E(\theta_i, \phi_i)} E(\theta_i, \phi_i)dA_s \frac{\cos(\phi_s)dA_c\cos(\phi_c)}{R_{sc}^2} \tag{3}$$

$$d\Phi_c = \text{BRDF}(\theta_i, \phi_i; \theta_C, \phi_C)d\Phi_s(\theta_i, \phi_i)d\Omega_{sc}\cos(\phi_s) \tag{4}$$

$$d\Phi_c = \text{BRDF}(\theta_i, \phi_i; \theta_c, \phi_c)d\Phi_s(\theta_i, \phi_i)\text{GCF}_{sc}\,\pi \tag{5}$$

$E(\theta_i, \phi_i)$ is the incident irradiance on the source section dA_s. GCF_{SC} is the projected solid angle from the source to the collector divided by π.

The GCF is independent of the first two terms and solely determined by the geometry of the system, including obscurations. The first term, BRDF $(\theta_i, \phi_i; \theta_c, \phi_c)$, is the bidirectional reflectance distribution function. It is usually considered independent of the second term, the incident power, and is therefore a function of the surface characteristics only. When reducing stray radiation propagation, one or more of these terms must be reduced. If any one of these terms is reduced to zero, no power will be transferred between the source and collector.

Stray Radiation Paths

Since the third term (GCF) in Eq. (4) is the *only* term that can be reduced to *zero*, it should receive attention first. This is a crucial point in a stray light analysis. Therefore, the logical starting place for stray light reduction is with the critical objects, since it is the GCF terms for these transfers which can be reduced to zero. Most novice analysts make the mistake of working on the BRDF term first.

$$\text{GCF} = \frac{\cos(\phi_s)dA_c\cos(\phi_c)}{\pi R_{sc}^2}$$

The apparent possibilities for decreasing the GCF are to increase R_{sc}, ϕ_s, ϕ_c or to reduce the area dA_c. Not readily apparent is that the GCF is limited by apertures and obstructions. These features will, in some cases, block out the entire view of the source section from the collector so that there is no direct path. This is the mathematical basis for the logical approach, discussed at the beginning of the chapter. First block off as many direct paths of unwanted energy to the detector as possible, and then minimize the GCF for the remaining paths.

Point Source Transmittance Definitions

There are five common ways to define the merit function of the stray light in an optical sensor. The most common and preferred method is to define it as the output irradiance divided by the input irradiance, in terms of the *normalized detector irradiance* (NDI),[30] or in terms of the *point*

source normalized irradiance transmittance (PSNIT).[31] This merit function is appropriate because it describes an irradiance transmittance, and it is relatively independent of the detector size.

A term often used in the past was the *off-axis rejection* (OAR), defined as the detector power divided by the input power from the same source *on-axis*. The term *rejection* is a misnomer because by definition the term describes a power transmittance, which can have little correlation with the rejected stray light. The second objection is that as a merit function it varies significantly with the detector size. If you double the area of the detector, the OAR will increase by about the same factor even though the system hasn't performed significantly worse in any way.

Another term commonly used is the system's stray light *point source power transmittance* (PSPT), or its reciprocal, the *attenuation* of the system. The PSPT is the detector power divided by the input power into the sensor from the specified *off-axis angle*. Again, this term varies with the detector size. Sometimes there is no well-defined entrance port so the denominator is impossible to define. Note that the magnitude of attenuation would normally be expressed in terms of a positive exponential. Beware that attenuations are often incorrectly called out with negative exponents.

A final PST definition that is sometimes specified is the *point source irradiance transmittance* (PSIT), defined as the output irradiance divided by the entrance port input irradiance. This definition becomes inappropriate when there is no clearly defined entrance port.

Surface Scattering Characteristics

Of the three potentially important factors in scattered radiation analysis cited above (the radiance of the undesirable source or sources, the geometry of the scattered radiation paths (GCF), and the surface scattering characteristics, (BRDF)), usually the first possibility considered is to improve the surface coatings or the addition of vane structure. In concept it *appears* to be the right place to start and that it is straightforward. Neither is the case; the BRDF never goes to zero as does the GCF, and the BRDF varies with input and output angles. However, with accurate *bidirectional reflectance distribution function* (BRDF) data and knowledge about the variations with applications, time, wavelength, and other factors, BRDF problems can be dealt with. The scattering characteristics of surfaces are discussed by Church, and the scattering characteristics of black coatings by Pompea and Breault elsewhere in this *Handbook*. The addition of vane sections on baffles can usually be considered as a specialized "coating" with its own specialized BRDF.

BRDF Characteristics

Usually, BRDF data that are presented represent only one profile of the BRDF, and many such profiles for various angles of incidence are necessary for understanding the scattering characteristics. However, studies have shown that a single profile of a mirror's surface scattering characteristics can be used, with some approximations, to define the BRDF for all angles of incidence.[32] This is a significant achievement. It reduces the amount of data that must be taken, and it makes it easier to calculate, or estimate, the BRDF value for any set of input and output angles. The BRDF can also be reconstructed for cases where only a single profile of the function has been presented, which has been the usual practice.

The approximation has its limitations, as clearly detailed by Stover.[33] The approximation is quite good for nominal angles of incidence (see Fig. 34).[34] However, it breaks down for very high θ_i and high observation angles θ_0.

It is important to understand qualitatively the scattering characteristics of diffuse black coatings. Figure 35 shows the BRDF profile of Martin Black at 10.6 μm for several angles of incidence.[35] At near-normal angles of incidence the BRDF values are bowl-shaped; the values increase at large observation angles from the normal. At high angles of incidence the BRDF values in the near specular direction have increased by 2.5 orders of magnitude. There is a good discussion of the qualitative characteristics of diffuse black surfaces by Pompea and Breault elsewhere in this *Handbook*.

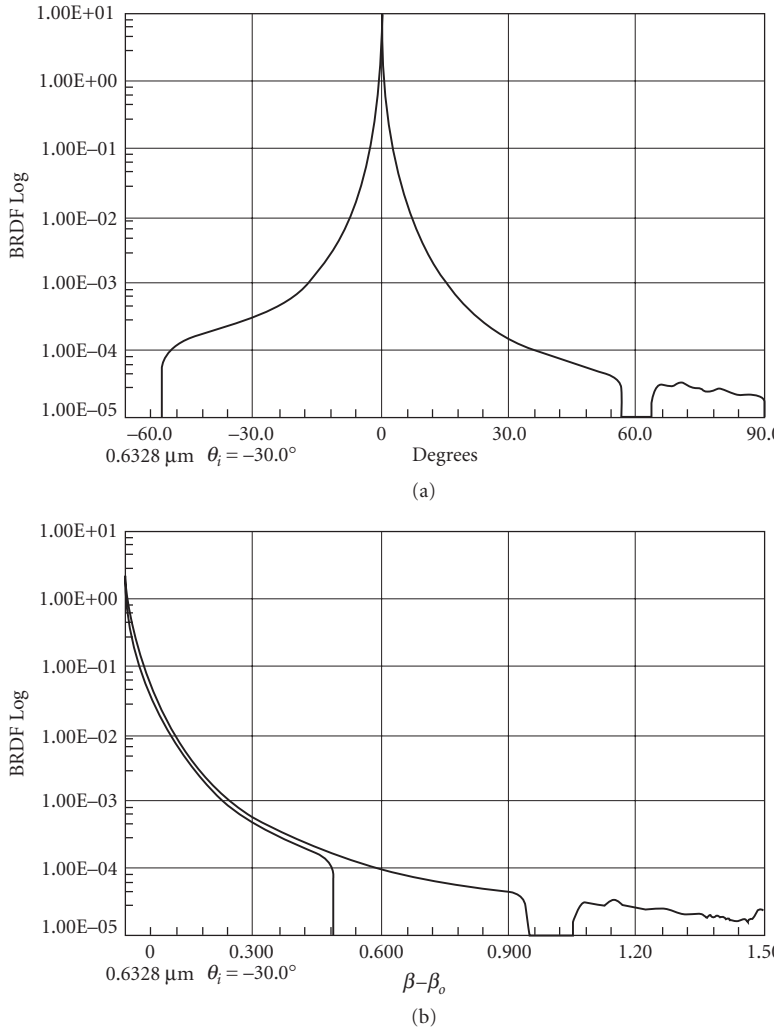

FIGURE 34 (*a*) The BRDF is asymmetrical when plotted against $\theta_s - \theta_i$, (*b*) The data in (*a*) exhibits near symmetry when plotted against $|\beta - \beta_o|$. The slight deviation from symmetry is due to the factor (cos $\theta_s Q$), where Q is a polarization factor. (*Ref. 34, p. 69, reprinted with permission.*)

7.4 OPTICAL SOFTWARE FOR STRAY LIGHT ANALYSIS

There is a small bevy of commercial optical software programs on the market that perform stray light analyses or some aspects of the stray light problems that are typically encountered. One must be knowledgeable of what each package can accomplish so the best thing to do is to ask for a demonstration of what each optical software manufacturer has to offer that is relevant to your design challenge. Here's a summary of a few commercially available optical software codes for stray light analysis. Note also that the programs' capabilities are always in a state of flux.

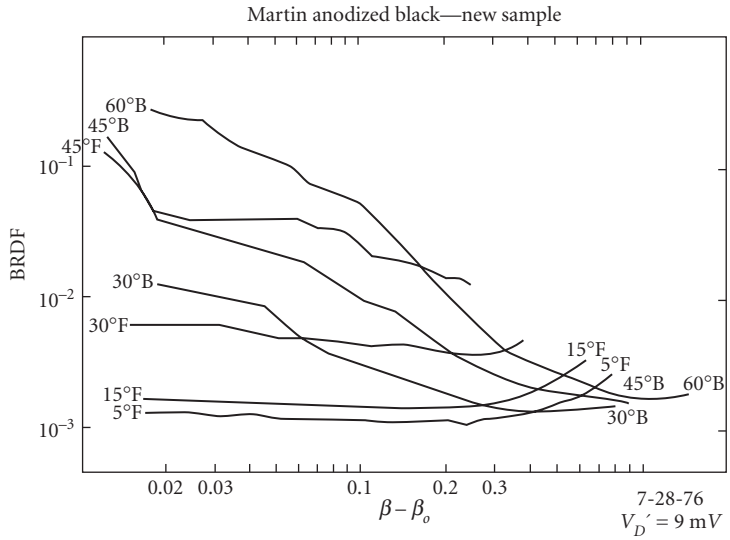

FIGURE 35 BRDF profile of Martin Black at 10 μm. (*F. O. Bartell et al., "A Study Leading to Improvements in Radiation Focusing and Control in Infrared Sensors," Final Report, Army Materials and Mechanics Research Center, December 1976.*)

ASAP, by Breault Research Organization, Inc.

ASAP Optical Software was developed to meet design and analysis criteria of imaging and illumination systems and the unique challenges of stray light analysis with CAD interoperability. ASAP is powered by the ASAP nonsequential ray-tracing engine—known throughout the optics industry for its accuracy and efficiency. Rays can encounter surfaces in any order and any number of times, with automatic ray splitting. Optimized for speed, ASAP will trace millions of rays in minutes. The standard edition of ASAP includes a license of the SolidWorks Parts Only 3D Modeling Engine—an intuitive 3D-design environment optimized for use with ASAP. The user can write ASAP geometry files from within SolidWorks, import XML files, or use BRO's proprietary smart-IGES system to import system models from any CAD package while maintaining fast, efficient ray trace speed.

Use ASAP to model complex imaging systems, illumination systems, and light-concentrating devices. Create highly accurate source models using source images, point sources, ray grids, and fans. Model incandescent bulbs, LEDs, CCFLs, and HID arc lamps, or import from the BRO Light Source Library. Perform the analyses necessary to validate your designs without experimental prototyping.

ASAP includes a distributed-processing capability allowing the user to complete big design and analysis jobs effectively in short-time span—spawn up to 5 additional ASAP sessions on other local area network (LAN), without leaving your desk. Web site: www.breault.com

FRED, by Photon Engineering

FRED is an optical engineering software package that uses a statistical ray sampling approach to analyzing incoherent stray light mechanisms in optical systems. The user can assign one or more of many different BSDF scatter functions to a surface. When a ray is incident on the surface, a specified number of scatter rays are generated in random directions into the hemisphere according to a uniformly random angular distribution, although a Monte-Carlo technique can be used

to generate scatter rays with directional ray density proportional to the BSDF function. The power assigned to any particular scatter ray is proportional to the incident ray power and value of the BSDF function evaluated in the direction of the scatter ray. Uniform sampling of angle space has the advantage that lower power scatter paths will be realized with higher probability. Ray-density direction sampling has the advantage that more rays are directed in the higher power directions which decreases the statistical noise in those directions.

When analyzing scatter from a surface, the user is often interested in only a subset of the entire hemispherical angular range. In these cases a technique called importance sampling can often be used to great advantage. The user can specify that the same number of scatter rays be generated into the importance sample direction as was originally directed into the hemisphere to decrease the statistical noise. An alternative is to decrease the number of rays but still achieve the same noise level. The desired angular range can be specified in a variety of ways and FRED will then direct scatter rays randomly into the specified range. The power assigned to each scatter ray is adjusted to account for the fact that it can be directed only into a subset of the entire hemisphere. Web site: www.photonengr.com

LightTools and CodeV, by Optical Research Associates

LightTools is a complete illumination design and analysis software product. It combines full optical accuracy, powerful optical and illumination analysis, and an intuitive graphical user interface in a 3D solid modeling environment where models interact with rays to produce virtual prototypes of manufacturable systems. A fully integrated illumination optimization capability automatically improves model performance. *LightTools*' Monte Carlo ray tracing facilitates accurate spectral modeling of the illuminance, luminance, intensity distributions, and CIE colorimetric data anywhere in the optomechanical model.

In addition to illumination system design, *LightTools* supports many other applications, from packaging studies to stray light analysis. For example, its ray path visualization collects and displays information about ray-surface interactions to identify system elements that are contributing to light loss, scatter, unintentional reflections, or ghost images. A unique point-and-shoot ray tracing capability allows rapid, interactive evaluation of optical behavior.

CODE V is used for the optimization, analysis, and tolerancing of image-forming optical systems and free-space photonic devices. Its many capabilities include powerful local and global optimization for optics, fast wavefront differential tolerancing that allows as-built considerations to be evaluated throughout the design process, and highly accurate diffraction beam propagation analysis. For stray light applications, CODE V can be used to analyze ghosts in imaging systems due to Fresnel reflections. Web site: www.opticalres.com

ZEMAX, by ZEMAX Development Corporation

The ZEMAX program, from ZEMAX Development Corporation, has two modes of use. Its primary use is as a sequential optical design (optimization) program. In this mode it has tools to help identify location of ghost pupils and images resulting from Fresnel reflections. A separate nonsequential mode has many capabilities necessary for stray light analysis, including scatter modeling with importance sampling.

ZEMAX's Nonsequential ray-tracing capabilities can further be extended to finding rays which have specific characteristics or properties. For example, imagine you are studying the stray light in a telescope:

How significant are rays which "ghost" reflected off of various surfaces (both mechanical and optical)?

Rays which are experience multiple reflections may be important, but how significant are those which experience more than four reflections?

How effective is a strategically placed baffle in terms of limiting the amount of stray light on the detector?

Website: www.zemax.com

TracePRO, by Lambda Research Corporation

TracePro, from Lambda Research Corporation, is a 3D Computer Aided Design (CAD) program for simulating the performance of illumination and optical systems. TracePro can model the propagation of light in imaging and nonimaging optomechanical systems. Models are created by combining imported lens designs, imported CAD geometry (IGES, STEP, SolidWorks, Pro/E, CATIA, or Inventor files), and geometrical objects created using TracePro's user interface. Optical properties are then assigned to each solid and surface using the TracePro interface or through the TracePro Bridge for SolidWorks. Source models are added by specifying grids, surface emitters, ray file data or by using the surface source utility. Rays are ray traced through the model, while keeping track of absorption, specular reflection and transmission, fluorescence and scatter at each intersected surface or volume scatter site.

From TracePro models, the user may ray trace and analyze:

- Light distributions in illumination and imaging systems
- Stray light, scattered light, and aperture diffraction
- Throughput, loss, or system transmittance
- Flux or power absorbed by surfaces and bulk media
- Light scattering in biological tissue
- Polarization effects
- Fluorescence effects
- Birefringence effects
- Lit Appearance

Website: www.lambdares.com

SPEOS, by Optis

OPTIS' simulation software family, SPEOS and OptisWorks. It manages and optimizes many of the optical aspects of a broad range of sensors: reflection, refraction, scatter from surfaces, diffraction, absorption, polarization, and Gaussian beam propagation. It calculates stray light, illumination, and realistic optical simulations. Any product that needs to manage interactions of light and surfaces is calculated. It deals with the various types of light sources also. The simulations limit the need for costly prototyping of systems.

OPTIS simulation software allows the designer to "see" and realistically render products to depict what the final performance of the illuminator will look like in its applied application with stunning similarity. Its software produces a unique and accurate physiological human vision model of the final lit product for comfort, safety, and performance.

7.5 METHODS

There are two distinct methods that have been used to evaluate a system for stray radiation. You can either build the system and test it, or you can model the system and try to predict its performance. Both methods have advantages and disadvantages. Taken *together* the two methods provide the means to ensure that the system will perform as desired.

Build-and-Test Approach

A common approach is to make the system and either use it or test it for stray radiation rejection. Certainly if the system consistently performs satisfactorily *in its operational environment*, it has passed the ultimate test. But what if it does not meet the desired or expected level of performance? Making more systems to test becomes expensive rapidly. In fact, for very large systems, usually only modifications ("fixes") can be contemplated because of the high cost. This is not the only argument against the build-and-test approach. The tests are rarely designed to determine *how* the scattered radiation is propagating through the system and which surfaces contribute most of the undesired radiation.

It is this information, and a thorough knowledge of the surface scattering characteristics, that is necessary to make measurable improvements to the system. Such a test, when determining the propagation paths, should yield information about how the system is reacting to its *test* environment, including the test equipment. Unless the tests are being conducted in the environment for which the system was designed, it is imperative to determine that the *test* environment is not giving erroneous results (either better or worse). Without analyzing the test configuration, you should expect that the environment *will* affect the system stray light measurements. It is also incorrect to assume that the test environment can only add to the stray light background. It is sometimes assumed that if the system passes the stray light tests in the lab it will only perform better in space or wherever its intended environment is. This is not necessarily true.

Now that several points have been made about the difficulty of making valid experimental tests, it must be stated that valid tests can and should be made. The measurement costs need not be prohibitive. Even relatively large optical systems have been fabricated and then modestly redesigned. Changes to the system can be made until the desired information and stray radiation rejection is attained. In some cases it will be less expensive to test an existing system and modify it if necessary than to analyze the system with computer software.

The system-level test need not be extensive; it is not necessary to have an all-encompassing measurement from on-axis to 90° off-axis. Indeed, few facilities are capable of making such tests when the attenuation gets even modestly high. An important point to recognize is that the most important paths to check are those at the nearer off-axis angles where the attenuation is not so high. These can usually be measured reliably.

At small off-axis angles the stray light noise is more often much higher than the detector background noise, while at the higher off-axis angles the stray light noise is well below the electronic/detector noise. From a performance point of view, at the higher off-axis angles there is usually only one additional scattering object (scatter from the main baffle) before these same near off-axis angle paths are encountered or are reinvolved. The validation of the analysis will only be susceptible to the scatter from this one object that can't be fully tested at the system level, but most of the scatter paths, and usually all the most important ones, will have been validated by the near off-axis measurements.

This one additional surface scatter most often (especially on space-based sensors) involves the vanes on the main baffle that shields the primary objective. It will normally reduce the optical noise incident upon it by four to five orders of magnitude. That's why the optical noise goes dramatically below the electronic noise. Its most important role is to occult the direct illumination of the objective which is usually part of the most significant direct scatter path. The performance of this baffle and its vane structure could be analyzed separately and then measured independently to confirm that it too will perform as predicted.

NOTE: Contrary to some published papers you cannot, in general, multiply the stray light transmittance of two parts of a sensor and determine the system's overall performance. Although the main baffle system can be analyzed (or measured) independently from the rest of the system, it is not correct to take its performance and multiply it times the stray light performance of the rest of the system. The stray light propagation paths are far more important than the magnitudes of the two parts. In the above analysis where it was proposed that the main baffle could be measured independently it was to confirm its performance alone. A full-system stray light analysis was assumed.

CONTROL OF STRAY LIGHT

Computer Analysis

As with the experimental tests, computerized analyses are also subject to errors. The three most significant ones are software limitations, scatter data of samples (not the real system), and user error. No software is capable of putting in every detail of a complex design, yet the computer model must faithfully represent the actual performance of the system. On the other hand, the software can put in "parts" with far greater mathematical precision than these parts can actually be assembled. Unless special studies are made the analyst does not usually account for assembly errors that might affect the actual system. The scatter characteristics of the surfaces, usually defined in terms of the bi-directional reflectance distribution function (BRDF), are usually measured on sample substrates, and controls must be exercised to ensure that the samples tested represent the sensor's actual coatings, and that they do not change with time. The stray light analysis programs are also subject to errors in determining the significant paths. The experimental test is for the actual design, with real coatings, and will include any extraneous unintentional paths due to misalignment or other causes.

On the positive side, a software program can point out many flaws in the system that contribute stray radiation by considering the input BRDF characteristics of the coatings. A program can also do trade-off studies, parametric analysis, and in many other ways aid in the study of alternate designs. The analysis of the paths of scatter will suggest meaningful modifications and help to discard impossible designs. These analyses allow designers to test designs and make modifications before the design goes into production. This is very useful, since rejecting a sensor design is much easier when it is on paper than after it has already been built. It is usually much more cost-efficient than cutting new hardware, redesigning the system, or making fixes on the built system.

If you are in a field related to the optical design of a sensor, be it at the design level or the system level, you know that it would be preposterous to perform the optical design analysis and then put the system together without testing it for its image quality. Yet that is how far the pendulum has swung in favor of performing a stray light analysis over making a system-level stray light test. It reflects a major change in attitude since the early 1970s. It has been stated by stray light analysts that the reliability of a stray light analysis is now much higher than experimental test results, so some people avoid the latter. While there is a degree of truth in this statement, it is wrong to omit the stray light test at the system level.

The advantages and disadvantages of the two methods are summarized in Fig. 36. The disadvantages of the build-and-test approach are the strengths of the analysis method, whereas the strengths of the build-and-test approach cover the weaknesses of an analysis. Taken together these two methods give the greatest amount of reliable information which you can use to create the optimal system and have confidence in its performance. Jointly, they indicate the reliability of the analysis and test results.

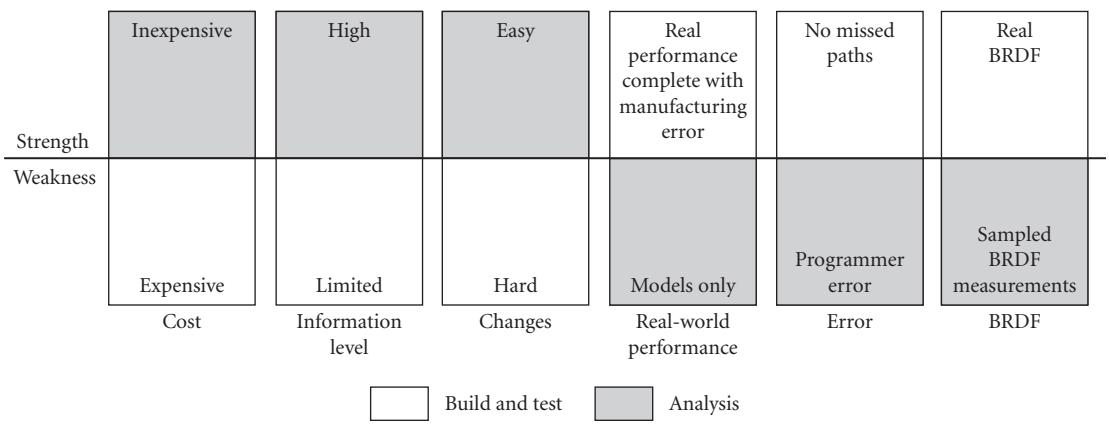

FIGURE 36 Build-and-test and analysis methods complement each other.

7.6 CONCLUSION

In summary, the issues involved in designing a system with stray light suppression in mind are

- **I.** System design concepts
  - **A.** Critical objects seen by the detector
  - **B.** Illuminated objects
  - **C.** Lyot stops
  - **D.** Field stops
  - **E.** Optical designs
- **II.** Baffle and vane design
  - **A.** Diffuse and specular vane cavities
  - **B.** Vane edge scatter
- **III.** Diffraction
- **IV.** Strut design
- **V.** Scattering theory
- **VI.** BRDF data
  - **A.** Log BRDF versus θ
  - **B.** Log BRDF versus log $(\beta - \beta_o)$
  - **C.** Polar plots
  - **D.** Isometric projections (3-D characteristics)
- **VII.** Coatings
  - **A.** Paints and anodized surfaces
  - **B.** AR coatings and other thin films
  - **C.** Mirror coatings
- **VIII.** Thermal emission
- **IX.** Ghost images
- **X.** Software
- **XI.** Detection, prevention, and removal of contamination

A step by step procedure that can help you to improve your system is:

- **I.** Start from the detector and identify what objects, called "critical objects," can be seen from various positions on the detector. Be sure to include a point near the edge of the detector.
- **II.** Work to remove the number of critical objects that the detector can see.
- **III.** Determine what objects the source of unwanted radiation can see, called the "illuminated objects."
- **IV.** If possible, reduce the number of illuminated objects seen.
- **V.** If there are illuminated objects that are also critical objects, work very hard on these paths. Orders of magnitude in improvement will be your reward.
- **VI.** If task V is not possible, then the computations are quite easy.
  - **A.** Calculate the power incident on the illuminated/critical objects.
  - **B.** Use Eq. (1) to calculate the transfer of power from the critical objects to the detector. Remember to properly account for the input and output angles when calculating the BRDF. *Do not* use a straight lambertian scatter distribution; there is no such distribution in reality.
- **VII.** Find all the paths connecting the illuminated objects to the critical objects.
- **VIII.** Evaluate the corresponding input and output angles at the illuminated and critical objects.

IX. Determine if vane structure will help, or if some other redesign will effectively block these paths.

X. For the calculated input and output angles, evaluate which coating would be lowest.

XI. Perform the stray light calculation using Eq. (1) in an iterative fashion. This should determine the most significant stray light path and quantify the amount of stray light on the detector

XII. Perform the above tasks for a series of off-axis positions of the point source.

7.7 SOURCES OF INFORMATION ON STRAY LIGHT AND SCATTERED LIGHT

J. D. Lytle and H. Morrow (eds.), "Stray Light Problems in Optical Systems," *Proc. SPIE*, vol. 107, April 18–21, 1977 (22 papers).

M. Kahan (ed.), "Optics in Adverse Environments," *Proc. SPIE*, vol. 216, Feb. 4–5, 1980 (30 papers).

G. H. Hunt (ed.), "Radiation Scattering in Optical Systems," *Proc. SPIE*, vol. 257, Sept. 30–Oct. 1, 1980 (28 papers).

S. Musikant (ed.), "Scattering in Optical Materials," *Proc. SPIE*, vol. 362, Aug. 25–27, 1982 (28 papers).

R. P. Breault (ed.), "Generation, Measurement, and Control of Stray Radiation III," *Proc. SPIE*, vol. 384, Jan. 18–19, 1983 (15 papers).

R. P. Breault (ed.), "Stray Radiation IV," *Proc. SPIE*, vol. 511, Aug. 23, 1984 (14 papers).

R. P. Breault (ed.), "Stray Radiation V," *Proc. SPIE*, vol. 675, Aug. 18, 1986 (46 papers).

R. P. Breault (ed.), "Stray Light and Contamination in Optical Systems," *Proc. SPIE*, vol. 967, Aug. 17–19, 1988 (33 papers).

J. C. Stover (ed.), "Scatter from Optical Components," *Proc. SPIE*, vol. 1165, Aug. 8–10, 1989 (42 papers).

R. P. Breault (ed.), "Stray Radiation in Optical Systems," *Proc. SPIE*, vol. 1331, July 12–13, 1990 (29 papers).

J. C. Stover (ed.), "Optical Scatter: Applications, Measurement, and Theory," *Proc. SPIE*, vol. 1530, July 21–27, 1991.

R. P. Breault (ed.), "Stray Light and Contamination in Optical Systems II," *Proc. SPIE*, vol. 1753, July 21–23, 1992.

F. O. Bartell et al., "A Study Leading to Improvements in Radiation Focusing and Control in Infrared Sensors," *Final Report Prepared for Army Materials and Mechanics Research Center*, December 1976.

J. A. Gunderson, "Goniometric Reflection Scattering Measurements and Techniques at 10.6 Micrometers," M.S. thesis, University of Arizona, 1977.

P. J. Peters, "Stray Light Control, Evaluation, and Suppression," *Proc. SPIE*, vol. 531, January 1985.

T. W. Stuhlinger, "Bidirectional Reflectance Distribution Function (BRDF) of Gold-Plated Sandpaper," M.S. thesis, University of Arizona, 1981.

A. W. Greynolds, "Computer-Assisted Design of Well-Baffled Axially Symmetric Optical Systems," M.S. thesis, University of Arizona, 1981.

J. W. Figoski, "Interferometric Technique for the Reduction of Scattered Light," M.S. thesis, University of Arizona, 1977.

J. S. Fender, "An Investigation of Computer-Assisted Stray Radiation Analysis Programs," Ph.D. dissertation, University of Arizona, 1981.

D. A. Thomas, "Light Scattering from Reflecting Optical Surfaces," Ph.D. dissertation, University of Arizona, 1980.

R. P. Breault, "Suppression of Scattered Light," Ph.D. dissertation, University of Arizona, 1979.

P. R. Spyak, "A Cryogenic Scatterometer and Scatter from Particulate Contaminants on Mirrors," Ph.D. dissertation, University of Arizona, 1990.

F. O. Bartell, "Blackbody Simulator Cavity Radiation Theory," Ph.D. dissertation, University of Arizona, 1978.

L. D. Brooks, "Microprocessor-based Instrumentation for BSDF Measurements from Visible to FIR," Ph.D. dissertation, University of Arizona, 1982.

A. G. Lusk, "Measurements of the Light Scattering Profile of Small Size Parameter Fibers," M.S. thesis, University of Arizona, 1987.

K. Nahm, "Light Scattering by Polystyrene Spheres on a Conducting Plane," Ph.D. dissertation, University of Arizona, 1985.

G. W. Videen, "Light Scattering from a Sphere on or Near an Interface," Ph.D. dissertation, University of Arizona, 1992.

Y. Wang, "Comparisons of BRDF Theories with Experiment," Ph.D. dissertation, University of Arizona, 1983.

S. J. Wein, "Small-Angle Scatter Measurement," Ph.D. dissertation, University of Arizona, 1989.

J. M. Bennett and L. Mattsson, *Introduction to Surface Roughness and Scattering*, Optical Society of America, Washington, D.C., 1989.

J. C. Stover, *Optical Scattering Measurement and Analysis*, McGraw-Hill, Inc., New York, 1990.

7.8 REFERENCES

1. R. P. Breault, "Problems and Techniques in Stray Radiation Suppression," *Stray Light Problems in Optical Systems*, J. D. Lytle and Howard Morrow (eds.), *Proc. SPIE* **107,** 1977, pp. 2–23.
2. R. P. Breault, A. W. Greynolds, and S. R. Lange, "APART/PADE Version 7: A Deterministic Computer Program Used to Calculate Scattered and Diffracted Energy," *Radiation Scattering in Optical Systems*, G. Hunt (ed.), *Proc. SPIE* **257,** 1980, pp. 50–63.
3. R. V. Shack, "Analytic System Design with a Pencil and Ruler–The Advantages of the $y-\overline{y}$ Diagram," *Applications of Geometrical Optics*, *Proc. SPIE* **39,** 1973.
4. S. R. Lange, R. P. Breault, and A. W. Greynolds, "APART, A First-Order Deterministic Stray Radiation Analysis Program," *Stray-Light Problems in Optical Systems*, J. D. Lytle and H. Morrow (eds.), *Proc. SPIE* **107,** 1977, pp. 89–97.
5. Ibid., R. P. Breault, "Problems and Techniques in Stray Radiation Suppression."
6. R. P. Breault, "Vane Structure Design Trade–Off and Performance Analysis," *Stray Light and Contamination in Optical Systems*, *Proc. SPIE* **967,** 1988.
7. Ibid., S. R. Lange, R. P. Breault, and A. W. Greynolds, "APART, A First–Order Deterministic Stray Radiation Analysis Program."
8. Ibid., R. P. Breault, A. W. Greynolds, and M. A. Gauvin, "Stray Light Analysis with APART/PADE, Version 8.7."
9. Ibid., R. P. Breault, "Problems and Techniques in Stray Radiation Suppression."
10. Ibid., S. R. Lange, R. P. Breault, and A. W. Greynolds, "APART, A First–Order Deterministic Stray Radiation Analysis Program."
11. This section is a part of a more complete mathematical description of the process which can be found in R. P. Breault, "Vane Structure Design Trade–Off and Performance Analysis." (Ibid.)
12. R. P. Breault, "Vane Structure Design Trade-Off and Performance Analysis" (Ibid.) contains a more detailed description of the process.
13. Ibid., R. P. Breault, "Problems and Techniques in Stray Radiation Suppression."
14. R. P. Breault, "Suppression of Scattered Light," Ph.D. dissertation, University of Arizona, 1979.
15. Ibid., R. P. Breault, "Problems and Techniques in Stray Radiation Suppression."
16. J. Gunderson, "Goniometric Reflection Scattering Measurements and Techniques at 10.6 Micrometers," M. S. thesis, University of Arizona, 1977.
17. Ibid., R. P. Breault, A. W. Greynolds, and S. R. Lange, "APART/PADE Version 7: A Deterministic Computer Program Used to Calculate Scattered and Diffracted Energy."
18. Ibid., R. P. Breault, A. W. Greynolds, and M. A. Gauvin, "Stray Light Analysis with APART/PADE, Version 8.7."
19. E. R. Freniere and D. L. Skelton, "Use of Specular Black Coatings in Well-Baffled Optical Systems," *Stray Radiation V*, Robert Breault (ed.), *Proc. SPIE* **675,** 1986, pp. 126–132.

20. A. W. Greynolds, computer code ASAP, Breault Research Organization, Inc., 1992.
21. G. L. Peterson, S. C. Johnston, and J. Thomas, "Specular Baffles," *Stray Radiation in Optical Systems II*, Robert P. Breault (ed.), *Proc. SPIE* **1753,** 1992.
22. P. R. Spyak, "A Cryogenic Scatterometer and Scatter from Particulate Contaminants on Mirrors," Ph.D. dissertation, University of Arizona, 1990.
23. "Product Cleanliness Levels and Contamination Control Program," *MIL-STD-1246A*, Dept. of Defense, Global Engineering Documents, Santa Ana, Calif., 18 Aug. 1967.
24. R. Young, "Low–Scatter Mirror Degradation by Particle Contamination," *Optical Engineering* **15,** no. 6, Nov.–Dec. 1976.
25. J. E. Harvey, "Light-Scattering Characteristics of Optical Surfaces," Ph.D. dissertation, University of Arizona, 1976.
26. P. R. Spyak and W. L. Wolfe, "Scatter from Particulate Contaminated Mirrors," *Optical Engineering* **31,** no. 8, Aug. 1992, pp. 1746–1784.
27. M. G. Dittman, "Contamination Scatter Functions for Stray Light Analysis," *Optical System Contamination: Effects, Measurements, and Control VII*, P. T. Chen and O. M. Uy (eds.), *Proc. SPIE,* **4774,** 2002, pp. 99–110.
28. Contact Dierdre Dykeman at Rome Air Development Center for the best way to access the results of this work.
29. H. E. Bennett, "Reduction of Stray Light from Optical Components," *Stray Light Problems in Optical Systems*, J. D. Lytle and H. Morrow (eds.), *Proc. SPIE* **107,** 1977, pp. 24–33.
30. Name coined by D. Rock, Hughes Aircraft Co., El Segundo, Calif.
31. Name coined by R. P. Breault; this is the name most often used in an APART stray light analysis.
32. Ibid., J. E. Harvey, "Light-Scattering Characteristics of Optical Surfaces."
33. J. C. Stover, *Optical Scattering: Measurement and Analysis*, New York: McGraw-Hill, Inc., New York, 1990.
34. Ibid., J. C. Stover, *Optical Scattering: Measurement and Analysis*, p. 69.
35. Ibid., J. Gunderson, "Goniometric Reflection Scattering Measurements and Techniques at 10.6 Micrometers."